Diphenylphenacyl sulfonium salt as dual photoinitiator for free radical and cationic polymerizations

3 authors:

Kerem Kaya
Istanbul Technical University
26 PUBLICATIONS **72** CITATIONS

SEE PROFILE

Johannes Kreutzer
Nature Publishing Group
22 PUBLICATIONS **207** CITATIONS

SEE PROFILE

Yusuf Yagci
Istanbul Technical University
744 PUBLICATIONS **20,511** CITATIONS

SEE PROFILE

Some of the authors of this publication are also working on these related projects:

click chemistry View project

photoinduced processes View project

Diphenylphenacyl Sulfonium Salt as Dual Photoinitiator for Free Radical and Cationic Polymerizations

Kerem Kaya,[1] Johannes Kreutzer,[1] Yusuf Yagci [iD][1,2]

[1]Department of Chemistry, Istanbul Technical University, 34469 Maslak, Istanbul, Turkey
[2]Chemistry Department, Faculty of Science, King Abdulaziz University, Jeddah, Saudi Arabia
Correspondence to: Y. Yagci (E-mail: yusuf@itu.edu.tr)

ABSTRACT: Diphenylphenacylsulfonium tetrafluoroborate ($DPPS^+$ BF_4^-) salt possessing both phenacyl and sulfonium structural units was synthesized and characterized. $DPPS^+BF_4^-$ absorbs light at relatively higher wavelengths. The direct and sensitized initiation activity of the salt in both cationic and free radical photopolymerizations was investigated and compared with that of its analogue triphenylsulfonium tetrafluoroborate ($TPS^+BF_4^-$). Differential scanning photocalorimetry and conventional gravimetric studies revealed that $DPPS^+BF_4^-$ showed higher efficiency for direct and sensitized photopolymerizations of most of the monomers investigated. Although, principally both homolytic and/or heterolytic cleavage is possible, theoretical studies suggested that homolytic pathway is more favored for the generation of reactive initiating species. © 2017 Wiley Periodicals, Inc. J. Polym. Sci., Part A: Polym. Chem. **2017**, *00*, 000–000

KEYWORDS: calorimetry; cleavage reaction; cationic polymerization; free radical polymerization; phenacyl onium salts; photoinitiator; sensitization; sulfonium salts

INTRODUCTION Photopolymerization is currently one of the most important polymerization techniques in wide range of applications such as coatings, adhesives inks, printing, and microelectronics.[1–5] While most of the industrial applications of photocuring focus on free radical polymerization techniques, the cationic mode also receives considerable attention in industry and academia mainly due to its insensitivity to oxygen.[6] The further growth of such interest is strongly coupled to the development of initiators which fulfill requirements for specific applications. High curing speed, wavelength selectivity, low migration, and solubility are typically important criteria for successful application of initiators in industrial curing processes. Onium salts are known to initiate both free radical and cationic polymerizations.[7,8] Among them, iodonium,[9–14] pyridinium,[11,15] phosphonium,[16,17] and sulfonium salts[9,14,18,19] are most extensively used as initiators for cationic polymerization. The major drawback of onium type initiators is their low spectral response at high wavelengths. In attempt to extend the sensitivity to higher wavelengths, onium salts were combined in a two component system in conjunction with photosensitizers.[20–22] Onium salts can, thus, be activated by photosensitizers with favorable absorption characteristics in mechanistically different pathways involving electron transfer reactions in exciplexes,[23–25] charge transfer complex,[26] and with free radicals.[27,28] However, solubility, compatibility, migration, and cost make bi-component systems less attractive for industrial applications. Phenacyl salts are a class of onium salts that can overcome this problem to some extent by incorporating a chromophore group in the structure and slightly shifting the absorption to longer wavelengths.[29,30] They are easily synthesized by the reaction of phenacyl halides and the corresponding heteroatom nucleophiles and subsequent ion exchange with the sodium, potassium, or silver salt of a non-nucleophilic counter anion.[31] As presented on the example of phenacyl pyridinium salt (Scheme 1), cleavage occurs upon photolysis either homolytically to give a phenacyl radical and the corresponding heteroatom radical cation or heterolytically resulting in the formation of the phenacyl cation directly. In the former case, internal electron transfer also yields phenacylium cation. Thus, formed species were shown to initiate both free radical and cationic polymerizations.[32]

Several phenacyl sulfonium salts were previously designed and successfully used in free radical and/or cationic polymerization reactions.[33–37] However, due to the aliphatic and cyclic nature, limited spectral shift and efficiency was obtained. To combine advantages from phenacyl and aryl sulfonium structures, we herein report the synthesis and

Additional Supporting Information may be found in the online version of this article.
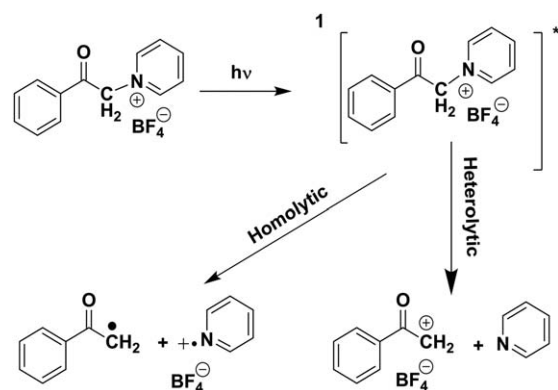
SCHEME 1 Photoinduced decomposition of phenacylpyridinium salts by homolytic and heterolytic cleavage.

characterization of a novel diphenylphenacyl sulfonium salt and its application as a dual initiator for radical and cationic photopolymerizations. Both direct and sensitized polymerizations were investigated and initiation efficiencies were compared with that of the analogous triphenyl sulfonium salt.

EXPERIMENTAL

Materials

Diphenyl sulfide (98%, Alfa Aesar), 2-bromoacetophenone (phenacylbromide, 99%, Merck), silver tetrafluoroborate (98%, Sigma-Aldrich), diphenyliodonium bromide, 97%, bis(2,4,6-trimethylbenzoyl)-phenylphosphineoxide (BAPO, Ciba specialty chemicals), 2,2-dimethoxy-2 phenylacetophenone (DMPA, Ciba), tetrabutylammonium hexafluorophosphate (98%, Sigma-Aldrich), and perylene (99%, Sigma-Aldrich) were used as received without further purification. Methyl methacrylate (MMA; 99%, Sigma-Aldrich) and styrene (St; 99%, Sigma-Aldrich) were purified by passing through a basic alumina column to remove the inhibitor before use. N-Vinylcarbazole (NVK; 98%, Sigma-Aldrich) was crystallized from absolute ethanol. Cyclohexene oxide (CHO) was purified by vacuum distillation over calcium hydride and stored under nitrogen. All solvents were purchased from Merck and purified by conventional procedures.

Instrumentation

^{1}H-NMR and ^{13}C-NMR spectra were recorded in deuterated chloroform (CDCl$_3$ with tetramethylsilane as an internal standard at 500 and 125MHz, respectively, on an Agilent VNMRS 500 spectrometer at 25 °C). Fourier-transform infrared (FTIR) spectra were recorded on Perkin–Elmer Spectrum One spectrometer with an ATR Accessory (ZnSe, PikeMiracle Accessory) and mercury cadmium telluride detector. Sixty-four scans were averaged. UV-visible spectra were recorded with a Shimadzu UV-1601 double-beam spectrometer equipped with a 50-W halogen lamp and a deuterium lamp which can operate between 190 and 1100 nm. Gel permeation chromatography (GPC) measurements were performed on a TOSOH EcoSEC GPC system equipped with an auto sampler system, a temperature controlled pump, a column oven, a refractive index (RI) detector, a purge, and degasser unit
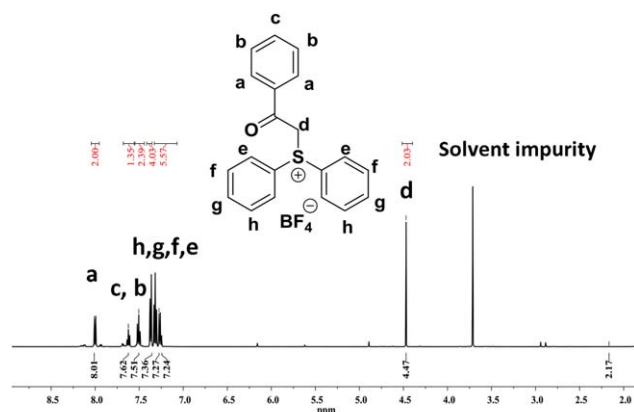

FIGURE 1 ^{1}H-NMR spectrum of DPPS$^+$BF$_4^-$.[Color figure can be viewed at wileyonlinelibrary.com]

and TSKgel superhZ2000, 4. 6 mm ID × 15 cm × 2 cm column. Tetrahydrofuran was used as an eluent at flow rate of 1.0 mL min^{-1} at 40 °C. RI detector was calibrated with polystyrene and poly(MMA) standards having narrow molecular-weight distributions. GPC data were analyzed using Eco-SEC Analysis software. The photo-differential scanning calorimetry (photo-DSC) measurements were carried out by means of a modified PerkinElmer Diamond DSC equipped with a high pressure mercury arc lamp emitting light at 320–500 nm. Cyclic voltammetry (CV) was performed on Princeton Applied Research VersaStat3 potentiostat under the control of VersaStudio Software with a three-electrode cell in a solution of 0.1 M tetrabutylammonium hexafluorophosphate (Bu$_4$N$^+$PF$_6^-$) dissolved in dry acetonitrile at a scan rate of 50 mV s^{-1}. The solution in the three-electrode cell was purged with pure nitrogen for at least 10 min before each measurement. A Pt (platinum) wire was used as the counter electrode and Ag/AgCl electrode was used as the reference electrode. LUMO energies were estimated by the empirical equation LUMO = $-(E_{red}^{onset} + 4.4)$ eV. The single crystal X-ray measurement was carried out on a Bruker D8 VENTURE diffractometer equipped with a shuterless detector using graphite monochromatic Mo-Kα radiation ($\lambda = 0.71073$ Å) and scanned with 1° Φ-rotation frames at room temperature.

Theoretical Calculations

Calculations were performed with the Gaussian09 program package.[38] Geometries were optimized with the M06 functional in combination with the 6–311G** basis set in gas phase. All geometries were confirmed as minimum structures displaying all frequencies real. Transition states were calculated with the Synchronous Transit-Guided Quasi Newton method as implemented in Gaussian09 using the optimized structures of the educt and product and a guess
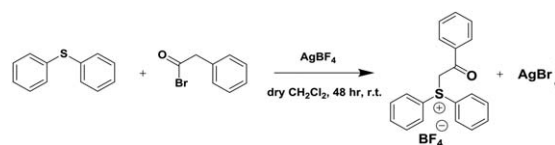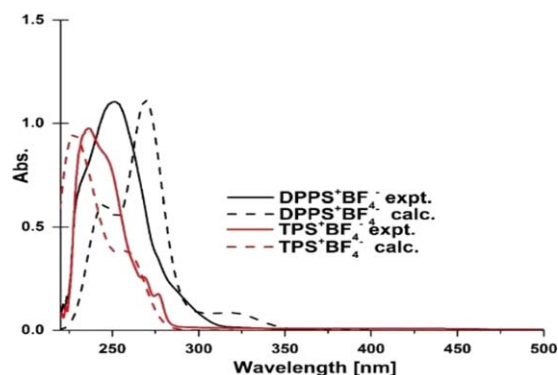

SCHEME 2 Synthesis of DPPS$^+$BF$_4^-$.

FIGURE 2 Calculated and measured UV-Vis spectra of $DPPS^+BF_4^-$ and $TPS^+BF_4^-$ (10^{-3} M in CH_2Cl_2). [Color figure can be viewed at wileyonlinelibrary.com]

structure for the transition state. The nature of the transition state was confirmed by displaying one imaginary frequency and connecting the educt, transition state, and product via an internal reaction coordinate calculation. Gibbs free energies and enthalpies include thermal corrections at 298 K. Excitation energies were calculated by density functional theory in its time dependent framework (TD-DFT) with the functional and basis set combination as described before. The spectra were modeled with a lorentzian broadening of each transition line with a half width of 0.18 eV.

Preparation of Triphenylsulfonium Tetrafluoroborate (TPS^+BF_4)

Triphenylsulfonium tetrafluoroborate ($TPS^+BF_4^-$) was prepared according to a known procedure[39] by reacting diphenyliodonium bromide with sodium tetrafluoroborate and diphenyl sulfide. Pure $TPS^+BF_4^-$ was obtained by recrystallization from ethanol in 85% yield.

Preparation of Diphenylphenacylsulfonium Tetrafluoroborate ($DPPS^+BF_4$)

Diphenylphenacylsulfonium tetrafluoroborate ($DPPS^+BF_4^-$) was prepared according to a known procedure.[40] Typically, a mixture

TABLE 1 Photoinduced Polymerization[a] Using $DPPS^+BF_4$ Photoinitiator for a Variety of Monomers

Monomer	Time (min)	Conversion[b] (%)	$M_n^c \times 10^{-3}$ (g mol^{-1})	$Đ^d$
MMA	15	25	22.26	1.27
MMA	30	56	37.62	1.78
MMA	60	64	25.13	2.42
MMA	120	68	26.75	1.71
St	120	59	11.43	2.42
NVK	120	52	1.39	5.19
CHO	120	31	26.40	1.85

[a] $\lambda_{max} = 300$ nm, solvent = dichloromethane, initiator = 0.07 mmol, and monomer = 4.7 mmol.
[b] Determined gravimetrically.
[c,d] Determined by GPC using polystyrene and poly(MMA) standards.

TABLE 2 Photoinduced Polymerization[a] Using TPS^+BF_4 Photoinitiator for a Variety of Monomers

Monomer	Time (min)	Conversion[b] (%)	$M_n^c \times 10^{-3}$ (g mol^{-1})	$Đ^d$
MMA	120	54	12.93	1.53
St	120	40	3.84	1.36
NVK	120	58	1.62	4.71
CHO	120	32	6.43	3.52

[a] $\lambda_{max} = 300$ nm, solvent = dichloromethane, initiator = 0.07 mmol, and monomer = 4.7 mmol.
[b] Determined gravimetrically.
[c,d] Determined by GPC using polystyrene and poly(MMA) standards.

of diphenylsulphide (5.0 g, 27 mmol), 2-bromoacetophenone (5.4 g, 27 mmol), and $AgBF_4$ (5.3 g, 27 mmol) was stirred in 100 mL of dry dichloromethane for 48 h at room temperature. After filtration, the solvent was removed to afford a tan-colored solid that could be recrystallized from dichloromethane. Single crystals suitable for single crystal XRD measurement were obtained by slow evaporation of a concentrated dichloromethane solution in 7 days.

Yield: 6.0 g (57%), (m.p. 160–161). FT-IR (ATR): $v = 1685(s)$, 2987(m), 3070(m). (Supporting Information Fig. S1). ^{1}H-NMR (500 MHz, CDCl$_3$, δ): 8.00 (dd, $J = 8.0$ Hz, 2H, Ar), 7.68 (t, $J = 7.60$ Hz, 1H, Ar), 7.50(t, $J = 7.50$Hz, 1H, Ar), 7.38–7.35 (m, 4H, Ar), 7.33-7.30 (m, 4H, Ar]), 7.26 (d, $J = 7.25$Hz, 2H, Ar), 7.24 (t, $J = 7.25$ Hz, 1H, Ar), 4.47(s, 2H, CH_2) ppm (Fig. 1). ^{13}C-NMR (125 MHz, CDCl$_3$, δ): 191.22 (C=O), 134.70 (C,Ar.), 135.94 (C, Ar) 134.00 (C, Ar), 129.39 (C, Ar), 126.93 (C, Ar.), 31.16 (C, CH_2). (Supporting Information Fig. S2).

General Procedure for Photoinitiated Polymerization
Before the polymerization trials, thermal and photochemical stabilities of the salts were investigated. Both salts are thermally stable up to 200 °C. UV-vis absorption changes in both photoinitiators under 300 nm light are presented in Supporting Information Figures S3 and S4. For a typical
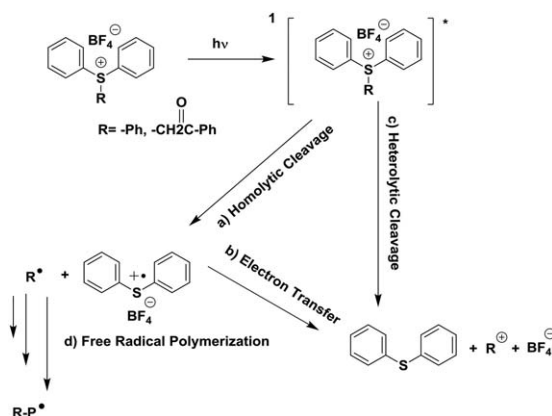
SCHEME 3 Initiation pathways for both radical and cationic polymerizations.
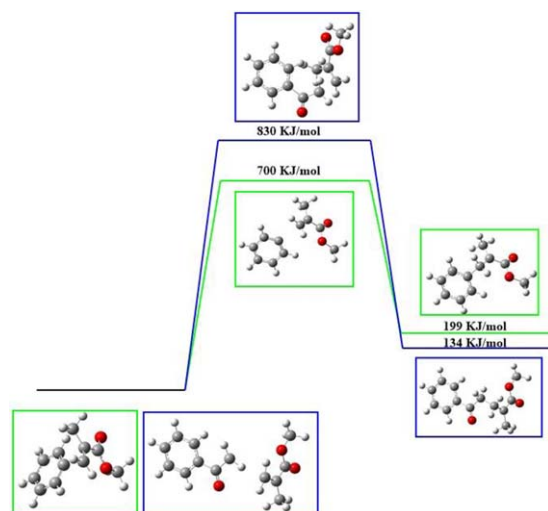
SCHEME 4 Energy diagram for the initiation of free radical polymerization reaction with MMA. [Color figure can be viewed at wileyonlinelibrary.com]

polymerization, a quartz tube with a magnetic bar was heated and degassed for 20 min before it was filled with monomer (0.5 mL, 4.7 mmol) and photoinitiator (0.07 mmol) in 0.5 mL dichloromethane under nitrogen. The solution was irradiated in a Rayonet photoreactor equipped with 12 lamps emitting at $\lambda = 300$ nm.

After irradiation, the solution was precipitated in 10-fold excess methanol and the precipitated polymer was filtered and dried under vacuum. All the photosensitized polymerization reactions of CHO were carried out in a capped borosilicate tube, the irradiation was achieved by a photoreactor equipped with six lamps emitting polychromatic light $\lambda = 400–500$ nm except DMPA sensitization in which lamps emitting light at 350 nm were used. For the photopolymerizations followed by photo-DSC, a uniform UV light intensity is delivered across the DSC cell to the sample and reference pans. The intensity of the light was measured as 62 mW cm^{-2} by a UV radiometer capable of broad UV range coverage. The mass of the sample was 3 mg, and the measurements were carried out in an isothermal mode at 30 °C under a nitrogen flow of 20 mL min^{-1}. The reaction heat liberated in the polymerization is directly proportional to the number of acrylate groups reacted in the system. By integrating the area under the exothermic peak, the conversion

of the acrylate groups (C) or the extent of the reaction was determined according to following

$$C = \Delta H_t / \Delta H_{0\ \text{theory}}, \qquad (1)$$

where ΔH_t is the reaction heat evolved at time t and $\Delta H_{0\ \text{theory}}$ is the theoretical heat for complete conversion. $\Delta H_{0\ \text{theory}} = 86$ kJ mol^{-1} for an acrylic double bond.[41]

RESULTS AND DISCUSSION

DPPS$^+$BF$_4^-$ was prepared by direct phenacylation process in one step, one pot (Scheme 2).

The structure of the salt was confirmed by NMR, IR, single crystal X-ray, and UV-Vis spectral analysis. As can be seen from Figure 1, the ^{1}H-NMR spectrum exhibits signals for the aromatic and methylene protons at 8.0–7.2 ppm and 4.4 ppm, respectively. The corresponding ^{13}C-NMR and FT-IR spectra also approve the expected structure (Supporting Information Figs. S1 and S2). In Figure 2, the calculated and experimentally measured UV-Vis spectra of the salts are compared. Notably, the absorption of the phenacyl salt appears at higher wavelengths.

Single Crystal X-Ray Crystallography

For single crystal XRD study, a single crystal of DPPS$^+$BF$_4^-$ with dimensions 0.01 × 0.04 × 0.20 mm was grown by slow evaporation of dichloromethane solution. The structure was solved by intrinsic method SHELXS-1997 (Sheldrick, 1997)[42] and refined with SHELXL-2014/7 (Sheldrick, 2014).[43] Molecular drawings are generated using OLEX2. Ver. 1.2-dev.[44] Thermal ellipsoids are plotted at the 50% probability level. The crystal and instrumental parameters were used in data collection. CCDC 1545578 contains the supplementary crystallographic data. Crystal parameters and refinement details for DPPS$^+$BF$_4^-$ are summarized in Supporting Information Table S5. Further details on crystal data, data collection, refinements, and oak ridge thermal ellipsoid plot (ORTEP) drawings with the atom numbering schemes are given in the Supporting Information (Supporting Information Figs. S6–S8).

The structure of the salt was further confirmed by single crystal XRD. The compound crystallized in the orthorhombic lattice system. The S—C bond lengths are in the normal range of 1.76–1.81 Å for a pyramidal sulfonium cation and lone pair repulsions of sulfur decrease the C—S—C bond

TABLE 3 Enthalpies (ΔH) and Gibbs Free Energies (ΔG) for the Different Reaction Pathways

	Pathway	TPS$^+$BF$_4^-$		DPPS$^+$BF$_4^-$	
		ΔH (kJ mol^{-1})	ΔG (kJ mol^{-1})	ΔH (kJ mol^{-1})	ΔG (kJ mol^{-1})
Homolytic cleavage	(a)	−250,43	−185,06	−203,81	−137,12
Electron transfer	(b)	58,83	58,80	2,83	3,39
Heterolytic Cleavage	(c)	117,88	230,05	108,50	222,58
Free radical polymerization	(d)	−246,62	−80,73	−176,04	−8,96
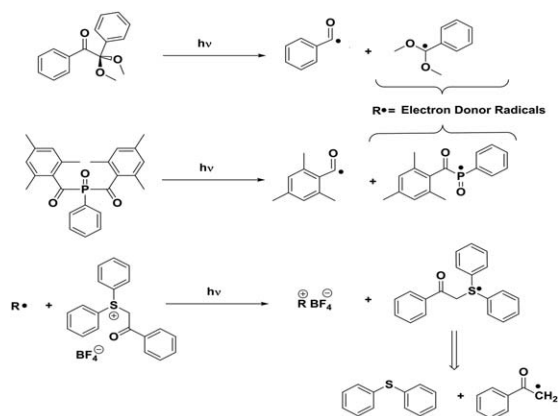
SCHEME 5 Initiation of free radical promoted cationic polymerization using DPPS$^+$BF$_4^-$.

angles below the tetrahedral values which are in the range of 102°–103° and in good agreement with the reported value for sulfonium cations.[45,46] The B—F bond lengths are in the range of 1.33–1.34 Å close to that given for BF$_4^-$ anion.[47] No inter- or intramolecular interaction in the crystal lattice could be observed.

To investigate the applicability of this photoinitiator in the initiation of radical polymerization, a series of vinyl monomers namely MMA, styrene (St), and NVK were used (Table 1). Polymerization of all monomers was successfully achieved and compared with the conventional sulfonium salt, TPS$^+$BF$_4^-$, relatively higher monomer conversions were attained (Table 2). It should be noted that NVK is a strong electron rich monomer and can undergo both free radical and cationic polymerizations. Interestingly, similar conversions were obtained for the cationic polymerization of the oxirane monomer, CHO that polymerizes only by a cationic mechanism indicating that the same cationic species were involved in the initiation process. The observed higher efficiency in the free radical process may be related to faster decomposition rate of the phenacyl salt. In the corresponding cationic mode, however, the initiating species are formed after the subsequent electron transfer process (*vide infra*).

Principally, the initiation action of phenacylium salts is based on either homolytic or heterolytic cleavage of the

excited salt. Homolytic cleavage (pathway a in Scheme 3) results in the formation of either a phenyl or a phenacyl radical, together with a diphenylsulfonium radical cation. The formed radical species are able to initiate the free radical polymerization in a further step [Scheme 3 (d)]. In the heterolytic cleavage pathway (pathway c in Scheme 3), diphenylsulfide and a phenyl cation are formed. The same products can, however, be obtained after homolytic cleavage (pathway a) followed by electron transfer from the radical species to the sulfonium radical (pathway b in Scheme 3). The cationic species obtained by heterolytic cleavage or homolytic cleavage with subsequent electron transfer are able to initiate cationic polymerization reactions. Furthermore, it is known that hydrogen abstraction from the solvent can generate H$^+$ which is able to initiate cationic polymerization.

We will start our discussion with the free radical polymerization reaction. Homolytic cleavage results in the formation of phenyl or phenacyl radicals and the diphenylsulfinyl radical. This reaction is exothermic for both, TPS$^+$BF$_4^-$ and DPPS$^+$BF$_4^-$ initiator; however, the formation of the phenyl radical is energetically slightly favored. Addition of the first MMA monomer unit either to the phenyl or phenacyl radical proceeds via a transition state which lies at 700 kJ mol^{-1} for the phenyl-MMA reaction and 830 kJ mol^{-1} for the phenacyl-MMA reaction (Scheme 4). The products of the first monomer addition lie energetically close to each other (199 kJ mol^{-1} for phenyl-MMA compared with 134 kJ mol^{-1} for phenacyl-MMA) with phenacyl-MMA being the energetically favored product. However, this might be one reason among others for the increased polymer conversion when DPPS$^+$BF$_4^-$ is used as initiator in the polymerization of MMA and St. The cationic polymerization mechanism can proceed via two pathways: homolytic cleavage and subsequent electron transfer results in the formation of phenacyl cations and diphenyl sulfide.

As outlined before, homolytic cleavage is energetically favored for the TPS$^+$BF$_4^-$ initiator. The electron transfer to diphenyl sulfide and formation of the respective cations is energetically disfavored for both the initiator species, however, energetically almost neutral for the DPPS$^+$BF$_4^-$ initiator.

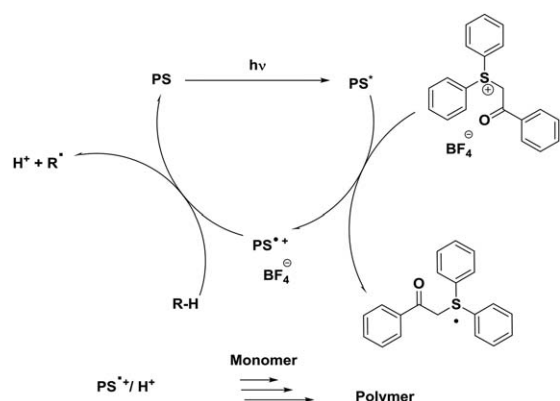**TABLE 4** Photosensitized Cationic Polymerization^a of CHO Using DPPS$^+$BF$_4$ and TPS$^+$BF$_4$

Initiator	Monomer	Sensitizer	Time (min)	Conversion^b (%)	$M_n^c \times 10^{-3}$ (g mol^{-1})	$Đ^d$
DPPS$^+$BF$_4^-$	CHO	BAPO	60	62	14.50	2.34
TPS$^+$BF$_4^-$	CHO	BAPO	60	45	21.00	2.12
DPPS$^+$BF$_4^-$	CHO	DMPA	60	42	16.02	1.82
TPS$^+$BF$_4^-$	CHO	DMPA	60	30	16.14	2.26
DPPS$^+$BF$_4^-$	CHO	Perylene	60	45	14.18	1.89
TPS$^+$BF$_4^-$	CHO	Perylene	60	38	37.83	1.39

^{a} λ = 350 nm for DMPA, 400—500 nm for BAPO and Perylene, solvent = dichloromethane, initiator = 0.07 mmol, sensitizer = 0.007 mmol, and monomer = 4.7 mmol.
^{b} Determined gravimetrically.
^{c,d}Determined by GPC using polystyrene and poly(MMA) standards.

SCHEME 6 Photosensitization of DPPS$^+$BF$_4^-$ salt for the initiation of cationic polymerization (PS: photosensitizer)

The second possibility, heterolytic cleavage seems energetically disfavored for both initiating systems. All reaction energies and enthalpies are summarized in Table 3. We, therefore, speculate that the initiation pathway in cationic polymerization proceeds via homolytic cleavage and subsequent electron transfer from the phenyl or phenacyl radical to the diphenyl sulfinium species. Energetically, the first step, which is the homolytic cleavage is favored for TPS$^+$BF$_4^-$; however, the second step, the electron transfer, proceeds more likely for the DPPS$^+$BF$_4^-$ initiator. The difference in the reaction enthalpies and reaction free energies between DPPS$^+$BF$_4^-$ and TPS$^+$BF$_4^-$ is rather small. Experimentally, this is reflected in similar conversions for the polymerization of CHO or NVK.

To further extend spectral sensitivity to longer wavelengths, indirect systems involving free radical promotion and sensitization by electron transfer reaction in the exciplex in cationic polymerizations by using CHO as a model monomer were conducted. DMPA, BAPO, and perylene were selected

as free radical source and sensitizer, respectively. As can be seen from Table 3, in all cases, DPPS$^+$BF$_4^-$ was found to be more reactive due to the more favorable thermodynamic conditions, as would be expected on the basis of their reduction potentials ($E_{1/2}^{red}$ (DPPS$^+$BF$_4^-$) = -0.60 eV, $E_{1/2}^{red}$ (TPS$^+$BF$_4^-$) = -1.10 eV). Upon irradiations at selected wavelengths, both DMPA and BAPO generate electron donor radicals that can readily be oxidized to the corresponding cationic species capable of initiating cationic polymerization of CHO (Scheme 5).

Similarly, with perylene as photosensitizer relatively higher conversions were attained (Table 4). According to Pappas et al., sensitization by polynuclear aromatic compounds proceeds via electron transfer processes within exciplexes[48] (Scheme 6). In our case, it is quite likely that the phenacyl radicals thus formed may further undergo electron transfer to generate additional cationic species.

Photo-DSC appeared to be very useful in investigating the initiation efficiency of initiators. We applied this method to shed light on the initiation efficiency of our initiators for the polymerization of a multifunctional monomer, namely, triethyleneglycol dimethacrylate (TEGDMA). Figure 3 shows the photo-DSC curves for the polymerization TEGDMA initiated by both TPS$^+$BF$_4^-$ and DPPS$^+$BF$_4^-$ under polychromatic light. The inset shows the plot of the conversion versus irradiation time derived from the polymerization system. It is clear that DPPS$^+$BF$_4^-$ polymerizes TEGDMA monomer in a shorter time with higher conversion in accordance with polymerization behavior observed for the monofunctional monomers.

CONCLUSIONS

A novel phenacyl-type sulfonium photoinitiator (DPPS$^+$BF$_4^-$) which is capable of initiating both radical and cationic polymerization was synthesized. DPPS$^+$BF$_4^-$ is thermally stable until 198 °C and showed higher absorption characteristics (Supporting Information Figures S3 and S4) with relatively higher polymerization conversions for most of the monomers compared with its triphenyl sulfonium analogue, TPS$^+$BF$_4^-$. Photosensitization studies also revealed that DPPS$^+$BF$_4^-$ gave higher conversions compared with that of TPS$^+$BF$_4^-$ probably due to the additional cationic species formed. CV studies revealed that DPPS$^+$BF$_4^-$ undergoes redox processes more efficiently due to the favorable thermodynamic conditions. Potential coating application of the initiating system was demonstrated by photo-DSC studies using a multifunctional monomer TEGDMA.
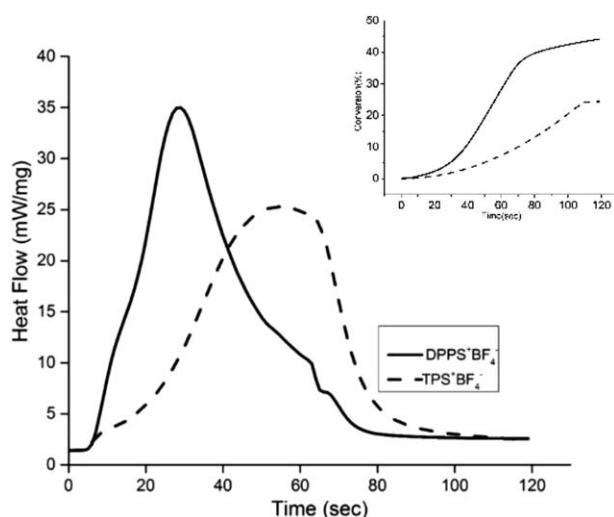

FIGURE 3 Photo-DSC profiles for the photopolymerization of TEGDMA irradiated at 30 °C by UV light (320–500 nm).

REFERENCES AND NOTES

1 N. S. Allen, *Photopolymerization and Photoimaging Science and Technology*; Elsevier Applied Science: London, **1989**.

2 J. P. Fouassier, *Photoinitiation, Photopolymerization, and Photocuring*; Hanser: München, **1995**.

3 S. Davidson, *Exploring the Science, Technology and Application of UV and EB curing*, SITA Technology Ltd: London, **1999**.

4 Y. Yagci, I. Reetz, *Prog. Polym. Sci.* **1998**, *23*, 1485.

5 J. P. Fouassier, Photochemistry and UV Curing: New Trends; Research Signpost, Trivandrum, **2006**.

6 O. S. Taskin, I. Erel-Goktepe, M. A. A. Khan, S. Pispas, Y. Yagci, *J. Photochem. Photobiol. A.* **2014**, *285*, 30.

7 J. V. Crivello, *Adv. Polym. Sci.* **1984**, *62*, 1.

8 M. Sangermano, *Pure Appl. Chem.* **2012**, *84*, 2089.

9 J. V. Crivello, J. H. W. Lam, *J. Polym. Sci. Part A: Polym. Chem.* **1980**, *18*, 2677.

10 J. V. Crivello, J. H. W. Lam, *Macromolecules* **1977**, *10*, 1307.

11 Y. Yagci, A. Kornowski, W. Schnabel, *J. Polym. Sci. Part A: Polym. Chem.* **1992**, *30*, 1987.

12 G. Hizal, Y. Yaĝci, W. Schnabel, *Polymer* **1994**, *35*, 2428.

13 J. V. Crivello, *Polym. Sci. Polym. Chem.* **1999**, *37*, 4241.

14 J. V. Crivello, J. H. W. Lam, *Macromolecules* **1979**, *10*, 1307.

15 Y. Yagci, T. Endo, *Adv. Polym. Sci.* **1997**, *127*, 59.

16 A. Onen, N. Arsu, Y. Yagci, *Angew. Macromol. Chem.* **1999**, *264*, 56.

17 L. Atmaca, I. Kayihan, Y. Yagci, *Polymer* **2000**, *41*, 6035.

18 J. V. Crivello, S. Kong, *Macromolecules* **2000**, *33*, 825.

19 S. Denizligil, Y. Yagci, C. M. Ardle, *Polymer* **1995**, *36*, 309.

20 M. Sangermano, J. V. Crivello, *ACS Symp. Ser.* **2003**, *847*, 242.

21 D. Dossow, Q. Q. Zhun, G. Hizal, Y. Yagci, W. Schnabel, *Polymer* **1996**, *37*, 2821.

22 G. Hizal, S. E. Emiroglu, Y. Yagci, *Polym. Int.* **1998**, *47*, 391.

23 J.-P. Fouassier, F. Morlet-Savary, J. Lalevée, X. Allonas, C. Ley, *Materials* **2010**, *3*, 5130.

24 C. Dursun, M. Degirmenci, Y. Yagci, S. Jockusch, N. J. Turro, *Polymer* **2003**, *44*, 7389.

25 Y. Yagci, A. Ledwith, *J. Polym. Sci. Part A: Polym. Chem.* **1988**, *26*, 1911.

26 J. Lalevee, M. A. Tehfe, F. Dumur, D. Gigmes, B. Graff, F. Morlet-Savary, J. Fouassier, *Macromol. Rapid Commun.* **2013**, *34*, 239.

27 M. Kara, S. Dadashi-Silab, Y. Yagci, *Macromol. Rapid. Comm.* **2015**, *36*, 2070.

28 M. Tehfe, F. Louradour, J. Lalevée, J. P. Fouassier, *Appl. Sci.* **2013**, *3*, 490.

29 Y. Yagci, Y. Y. Durmaz, B. Aydogan, *Chem. Rec.* **2007**, *7*, 78.

30 E. Takahashi, F. Sanda, T. Endo, *J. Appl. Polym. Sci.* **2004**, *91*, 3470.

31 A. Nese, S. Sen, M. A. Tasdelen, N. Nugay, Y. Yagci, *Macromol. Chem. Phys.* **2006**, *207*, 820.

32 M. A. Tasdelen, B. Karagöz, N. Bicak, Y. Yagci, *Polym. Bull.* **2008**, *59*, 759.

33 N. Yonet, N. Bicak, Y. Yagci, *Macromolecules* **2006**, *39*, 2736.

34 F. Kasapoglu, M. Aydin, N. Arsu, Y. Yagci, *J. Photochem. Photobiol. A.* **2003**, *159*, 151.

35 F. Kasapoglu, A. Onen, N. Bicak, Y. Yagci, *Polymer* **2002**, *43*, 2575.

36 Y. Y. Durmaz, O. Zaim, Y. Yagci, *Macromol. Rapid. Comm.* **2008**, *29*, 892.

37 J. V. Crivello, S. Kong, *J. Polym. Sci. Part A Polym. Chem.* **2000**, *38*, 1433.

38 M. J. Frisch, G. W. Trucks, H. B. Schlegel, G. E. Scuseria, M. A. Robb, J. R. Cheeseman, G. Scalmani, V. Barone, G. A. Petersson, H. Nakatsuji, X. Li, M. Caricato, A. Marenich, J. Bloino, B. G. Janesko, R. Gomperts, B. Mennucci, H. P. Hratchian, J. V. Ortiz, A. F. Izmaylov, J. L. Sonnenberg, D. Williams-Young, F. Ding, F. Lipparini, F. Egidi, J. Goings, B. Peng, A. Petrone, T. Henderson, D. Ranasinghe, V. G. Zakrzewski, J. Gao, N. Rega, G. Zheng, W. Liang, M. Hada, M. Ehara, K. Toyota, R. Fukuda, J. Hasegawa, M. Ishida, T. Nakajima, Y. Honda, O. Kitao, H. Nakai, T. Vreven, K. Throssell, J. A. Montgomery, Jr., J. E. Peralta, F. Ogliaro, M. Bearpark, J. J. Heyd, E. Brothers, K. N. Kudin, V. N. Staroverov, T. Keith, R. Kobayashi, J. Normand, K. Raghavachari, A. Rendell, J. C. Burant, S. S. Iyengar, J. Tomasi, M. Cossi, J. M. Millam, M. Klene, C. Adamo, R. Cammi, J. W. Ochterski, R. L. Martin, K. Morokuma, O. Farkas, J. B. Foresman, D. J. Fox, *Gaussian 09, Revision A.02*, Gaussian, Inc., Wallingford CT, **2016**.

39 F. M. Beringer, A. Brierley, M. Drexler, E. M. Gindler, C. C. Lumpkin, *J. Am. Chem. Soc.* **1953**, *75*, 2708.

40 M. Takatu, Y. Hayasi, H. Nozaki, *Tetrahedron* **1970**, *26*, 1243.

41 E. Andrzejewska, M. Andrzejewski, *J. Polym. Sci., Part A: Polym. Chem.* **1998**, *36*, 665.

42 G. M. Sheldrick, *SHELXL*; Universitaet Goettingen, Goettingen Germany, **1997**.

43 G. M. Sheldrick, *Acta. Cryst. A.* **2008**, *64*, 112.

44 O. V. Dolomanov, L. J. Bourhis, R. J. Gildea, J. A. K. Howard, H. Puschmann, *J. Appl. Chem.* **2009**, *42*, 339.

45 D. Zhao, Z. Fei, W. H. Ang, P. J. Dyson, *Int. J. Mol. Sci.* **2007**, *8*, 304.

46 A. P. Marchand, R. Kaya, S. W. Muchmore, D. van der Helm, *J. Org. Chem.* **1986**, *51*, 825.

47 H. Ishida, *J. Mol. Struct.* **2002**, *606*, 273.

48 S. P. Pappas, L. R. Gatechair, J. H. Jilek, *J. Polym. Sci. Polym. Chem. Ed.* **1984**, *22*, 77.